SIAM J. SCI. COMPUT.
Vol. 23, No. 1, pp. 170–192

VORTICITY-PRESERVING LAX–WENDROFF-TYPE SCHEMES FOR THE SYSTEM WAVE EQUATION*

K. W. MORTON† AND P. L. ROE‡

Abstract. In numerical solutions of fluid flow, vorticity can be generated by truncation errors. We analyze this phenomenon for linearized equations and give conditions for preventing it. The Lax–Wendroff method that meets these constraints is essentially unique, although there are two distinct interpretations, and also turns out to have optimal properties regarding stability and truncation error. The extension of the scheme to unstructured grids is given, together with some discussion of practical problems to which these schemes might bring improvement.

Key words. vorticity-preserving, system wave equation, discrete Kelvin's theorem

AMS subject classifications. 35B05, 35F05, 35L05, 35L65, 65M06, 76N10

PII. S106482759935914X

1. Introduction.

Much of computational fluid dynamics (CFD) is based on the analysis of simple "model problems." To an astonishing extent, the solution of problems governed by hyperbolic equations is based on analysis of the one-dimensional linear advection equation $u_t+au_x=0$. However, neither this nor the multidimensional $u_t+\vec{a}\cdot\nabla u=0$ really reflects the richness of fluid behavior, capturing merely advection and some aspects of wave propagation but ignoring, for example, all phenomena associated with vorticity, which are of vital importance in many three-dimensional situations.

The simplest model problem to combine wave propagation and vorticity is the system wave equation. We will write this in two space dimensions in the matrix form, using a notation corresponding to acoustic waves in a fluid that is stationary in the mean, with pressure p^* and velocity $\vec{u}^*=(u^*,v^*)$; thus

$$\partial_t \mathbf{u} + cL\mathbf{u} = 0. \tag{1}$$

Here $\mathbf{u}=(p^*/(\rho c^2),u^*/c,v^*/c)\equiv(p,u,v,)$, c is the sound speed in the mean flow, and

$$L=\begin{bmatrix} 0 & \partial_x & \partial_y \\ \partial_x & 0 & 0 \\ \partial_y & 0 & 0 \end{bmatrix}. \tag{2}$$

Restriction to two dimensions is merely for economy of notation; all of the analysis at the PDE level extends very straightforwardly to three dimensions, as does the numerical analysis on Cartesian grids. We study the wave equation in system rather than scalar ($\partial_{tt}u=c^2\nabla^2u$) form for two reasons: first, because this is the form of

*Received by the editors July 22, 1999; accepted for publication (in revised form) January 16, 2001; published electronically June 19, 2001.
http://www.siam.org/journals/sisc/23-1/35914.html

†Department of Mathematical Sciences, University of Bath, Bath BA2 7AY, UK and Oxford University Computing Laboratory, Oxford, UK (Bill.Morton@comlab.ox.ac.uk).

‡Department of Aerospace Engineering, University of Michigan, Ann Arbor, MI and Centre pour Mathematiques et Leurs Applications, Ecole Normale Supérieure de Cachan, France (philroe@engin.umich.edu).

the wave equation that is hidden inside the Euler equations, whether in their two-dimensional unsteady or in their three-dimensional supersonic steady forms [1], and second, because the scalar form automatically implies vanishing vorticity, whereas the interaction of the waves with vorticity is one of the aspects we want to study.

Here the interaction is very simple, as befits a model problem. We easily deduce from (1), (2), if c is a constant, that

$$\partial_t \zeta = 0, \qquad \text{where} \qquad \zeta = \partial_x v - \partial_y u.$$

In other words, there is no interaction, and any initial distribution of vorticity is preserved. Maintaining this independence at the discrete level will be one of our objectives. In section 6, however, we consider more general, variable coefficient, problems, for which vorticity is created by the interaction of waves with density gradients. In this case, there is a very satisfying discrete parallel.

It is a trivial modification to change the notation so that (1), (2) describe Maxwell's equations, and the constraint of invariant vorticity becomes one of invariant (and vanishing) divergence of the magnetic field. The two cases differ, however, when nonconstant coefficients are involved, a case that will be treated in due course. The analysis also applies to the divergence constraint in magnetohydrodynamics and to maintaining the div-curl identity when using a velocity-vorticity formulation of the Navier–Stokes equations.

We study fully discrete schemes because of our personal conviction that transient hyperbolic problems are most naturally treated by such methods. More specifically, we study Lax–Wendroff schemes because the Taylor expansion of the evolution operator seems to be the most general technique available, applicable to the wave equation for any order of accuracy. However, Lax–Wendroff schemes are ambiguous in more than one dimension. For example, if we look to discretize $u_t + \vec{a} \cdot \nabla u = 0$ to second-order accuracy on the standard nine-point stencil, we have only six constraints on the nine coefficients and hence three degrees of freedom. There are even more degrees of freedom in discretizing a system of equations. One reason for the rise of finite-element and finite-volume methodologies is that by working within a more disciplined framework some of the ambiguity is removed, hopefully without at the same time losing valuable options.

In the early stages of the present analysis we consider mainly regular rectangular grids with uniform spacing h in both x and y. We do not impose any particular interpretation on the discrete solution $u^n_{i,j}$: the values could represent cell-averaged quantities as in a cell-centered finite-volume scheme, or nodal values as in a vertex-centered finite-difference scheme. One point of interest is that by initially taking a simple finite-difference viewpoint, the formulae that emerge as having distinguished properties are precisely those that have dual interpretations as each of the above. Subsequently, however, we find that only the finite-volume interpretation generalizes to unstructured grids but that the particular form of finite-volume scheme to emerge is not the one most commonly encountered.

In section 2 of the paper, we recall some simple formulae of the finite-difference calculus and some elementary properties of the wave equation. In section 3 we place constraints on the scheme such that some discrete measure of vorticity is preserved and in section 4 show that requiring an adjoint property on a minimal stencil results in a unique version of the Lax–Wendroff scheme, although one having two distinct implementations. In section 5 we analyze the stability and truncation error of this scheme. In section 6 we show that if the waves are being propagated in a uniformly

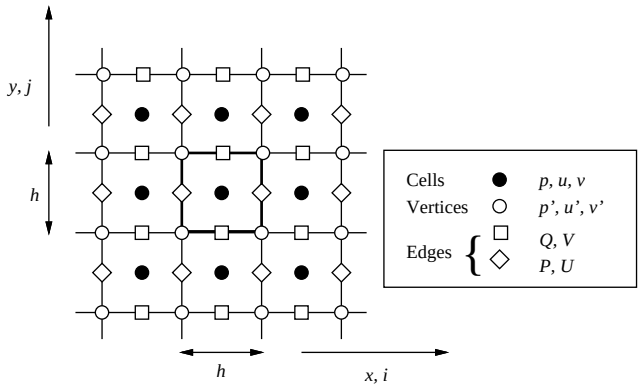

FIG. 1. *Grid definition.*

moving medium, then any vorticity present in the initial conditions will be propagated numerically according to the scalar version of our Lax–Wendroff method.

In section 7 we turn to irregular grids, and we find that there is still a measure of vorticity that is conserved, and in section 8 generalize further to the case of a problem with variable coefficients, although still linear. In this case the argument can be made global to yield a discrete Kelvin theorem.

2. Properties of the exact and discrete solution operators.

2.1. Discrete notation. As stated in the introduction, we concentrate at first on simple finite-difference formulations on uniform grids. These can be manipulated using a calculus that is almost as transparent as that of the differential operators. We exploit this simplicity to remove ambiguity from the finite-difference formulae by requiring certain algebraic properties. Then we ask what interpretations are compatible with the formulae.

We adopt a uniform square grid, such that the spacing in the x and y directions is h and the time step is Δt, with $u^n_{i,j}$ a discrete approximation located at $(x, y, t) = (ih, jh, n\Delta t)$. The standard discrete differencing and averaging operators are defined by

$$\delta_x()_{\cdot,\cdot} = ()_{\cdot+\frac{1}{2},\cdot} - ()_{\cdot-\frac{1}{2},\cdot}, \qquad \mu_x()_{\cdot,\cdot} = \tfrac{1}{2}\{()_{\cdot+\frac{1}{2},\cdot} + ()_{\cdot-\frac{1}{2},\cdot}\},$$

$$\delta_y()_{\cdot,\cdot} = ()_{\cdot,\cdot+\frac{1}{2}} - ()_{\cdot,\cdot-\frac{1}{2}}, \qquad \mu_y()_{\cdot,\cdot} = \tfrac{1}{2}\{()_{\cdot,\cdot+\frac{1}{2}} + ()_{\cdot,\cdot-\frac{1}{2}}\},$$

where it is understood that the result of any operator is located halfway between the two input points. Then the product $\Delta_{ox}()_{i,j} \equiv \mu_x\delta_x()_{i,j}$ is a central difference $\frac{1}{2}\{()_{i+1,j} - ()_{i-1,j}\}$ located at the grid point i, j, and the product $\mu_y\delta_x()_{i,j}$, which features frequently in what follows, involves four points $(i \pm \frac{1}{2}, j \pm \frac{1}{2})$ of a square centered at i, j.

The points with integer coordinates will be called *cells*, those with one integer and one half-integer coordinate *edges*, and those with two half-integer coordinates *vertices*. The variables stored at cells will be (p, u, v). The same variables stored at vertices will be distinguished by primes where necessary. The variables stored at vertical edges will be (P, U) and those stored at horizontal edges (Q, V), where both P and Q are approximations to the pressure. In a finite-volume interpretation the edge quantities are the fluxes (see Figure 1).

If it is recognized that each application of the above operators changes the centering of the mesh values to a different set of grid points, then arbitrarily long products of operators are allowed and all multiplications commute. It is simple to prove analogues of differential identities. For example, using $\langle \cdot, \cdot \rangle$ to denote an inner product,

$$\begin{aligned} \langle p, \delta_x U \rangle &\equiv \sum_{i,j} h^2 p_{i,j} \left(U_{i+\frac{1}{2},j} - U_{i-\frac{1}{2},j} \right) \\ &= -\sum_{i,j} h^2 \left(p_{i+1,j} - p_{i,j} \right) U_{i+\frac{1}{2},j} \quad \equiv \quad -\langle \delta_x p, U \rangle \end{aligned}$$

and a similar argument leads to $\langle p, \mu_x U \rangle = \langle \mu_x p, U \rangle$. Thence we have

$$\langle p, \mu_x \delta_x u \rangle \equiv \langle p, \Delta_{ox} u \rangle = -\langle \Delta_{ox} p, u \rangle, \quad \text{etc.}$$

Also we can combine cell and vertex values; for example,

$$\langle p, \mu_y \delta_x u' \rangle \equiv \sum_{i,j} \tfrac{1}{2} h^2 p_{i,j} (u'_{i+\frac{1}{2},j+\frac{1}{2}} - u'_{i-\frac{1}{2},j+\frac{1}{2}} + u'_{i+\frac{1}{2},j-\frac{1}{2}} - u'_{i-\frac{1}{2},j-\frac{1}{2}})$$

$$= -\sum_{i,j} \tfrac{1}{2} h^2 \left(p_{i+1,j+1} - p_{i,j+1} + p_{i+1,j} - p_{i,j} \right) u'_{i+\frac{1}{2},j+\frac{1}{2}} = -\langle \mu_y \delta_x p, u' \rangle.$$

Thus inner products are meaningful provided each term has the same centering. Such products may be called compatible. Matrix-valued operators will be a useful way to describe schemes, and obey the usual rules of matrix multiplication, provided each matrix has compatible entries.

2.2. Symmetry of solutions. An obvious property of (1), (2) is that because it involves only the divergence and gradient operators, then any solution remains a solution under an arbitrary translation or rotation of the (x, y)-plane. Clearly this cannot be true of the discrete solution, but we should insist on the weaker condition that the solution remains a solution under any translation or rotation that maps the grid onto itself.

This will ensure that all truncation errors are symmetric functions of the wave numbers k_x, k_y; it would also be a desirable property (minimizing the anisotropy of the scheme) if the leading terms depended only on $(k_x^2 + k_y^2)$.

2.3. Power series form. A formal solution to the initial-value problem for (1) is

$$\mathbf{u}(t) = \mathrm{e}^{-cLt} \mathbf{u}(0). \tag{3}$$

Let e^{-cLt} be represented by its power series, separating the odd and even terms,

$$\mathrm{e}^{-cLt} = 1 - \sum_{p=1}^{p=\infty} \frac{(cLt)^{2p-1}}{(2p-1)!} + \sum_{q=1}^{q=\infty} \frac{(cLt)^{2q}}{(2q)!}.$$

We can easily verify that

$$L(L^2 - \nabla^2) = 0,$$

which implies that

$$L^{p+2} = \nabla^2 L^p, \qquad p \geq 1. \tag{4}$$

Then we can write

$$\mathbf{u}(t) = \left[1 - (cLt)\sum_{p=0}^{p=\infty} \frac{t^{2p}(c^2\nabla^2)^p}{(2p+1)!} + (cLt)^2 \sum_{q=0}^{q=\infty} \frac{t^{2q}(c^2\nabla^2)^q}{(2q+2)!}\right] \mathbf{u}(0). \tag{5}$$

Truncating each sum at its first term will lead to a second-order Lax–Wendroff method. For extension to higher order it is useful to note that each term beyond the third merely represents continued applications of the Laplacian, either to L or to L^2. The structure of L is that its first row represents a divergence and its first column a gradient. As for L^2, we have

$$L^2 = \begin{bmatrix} \partial_x^2 + \partial_y^2 & 0 & 0 \\ 0 & \partial_x^2 & \partial_x\partial_y \\ 0 & \partial_x\partial_y & \partial_y^2 \end{bmatrix},$$

which displays the Laplacian and the grad-div operator. Most of these operators are ambiguous on the usual nine-point stencil of Lax–Wendroff schemes, and it is that ambiguity we seek to resolve.

2.4. Conservation form. In the cell-centered finite-volume method, discrete conservation is ensured by drawing a control volume around the grid point of interest and writing the update as an integral around this volume. In the generic case of a vector $\mathbf{U}$ of conserved variables, with fluxes $\mathbf{F}, \mathbf{G}$ in the (x, y)-directions, respectively, one has

$$h^2\left[\mathbf{U}^{n+1} - \mathbf{U}^n\right] + h\Delta t\left[\delta_x\mathbf{F}^* + \delta_y\mathbf{G}^*\right] = 0,$$

where $\mathbf{F}^*, \mathbf{G}^*$ are numerical fluxes evaluated from some formula to be determined. In the present case we can write, with $\nu = c\Delta t/h$ and following the notation of Figure 1,

$$p^{n+1} - p^n + \nu[\delta_x U + \delta_y V] = 0, \tag{6}$$

$$u^{n+1} - u^n + \nu\delta_x P = 0, \tag{7}$$

$$v^{n+1} - v^n + \nu\delta_y Q = 0. \tag{8}$$

It will usefully restrict the schemes to require that they can be written in this form. A second-order scheme of the Lax–Wendroff type follows from taking U, V, P, Q to be estimates halfway through the time step. However, we will find subsequently that it is a rather special type of conservation form that emerges from the analysis.

3. Preservation of discrete vorticity. We will now require that some discrete measure of vorticity is preserved during a time step. There are two simple measures.

3.1. Centered vorticity. First define the "centered vorticity"

$$\zeta_{\Delta_1} = \mu_x\delta_x v - \mu_y\delta_y u = Z_1\mathbf{u}, \tag{9}$$

where $Z_1 = [0, -\mu_y\delta_y, \mu_x\delta_x]$, and require that $\zeta_{\Delta_1}^{n+1} = \zeta_{\Delta_1}^n$, so that

$$\begin{aligned} 0 &= Z_1(\mathbf{u}^{n+1} - \mathbf{u}^n) \\ &= -\nu Z_1[\delta_x U + \delta_y V, \delta_x P, \delta_y Q] \\ &= \nu\delta_x\delta_y(\mu_y P - \mu_x Q). \end{aligned}$$

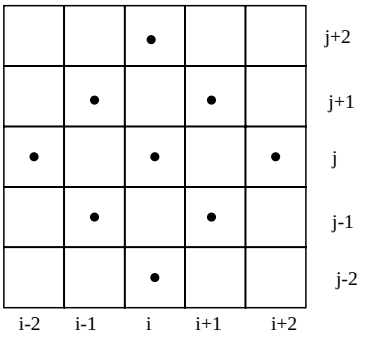

FIG. 2. *The stencil for Richtmyer's version of Lax–Wendroff.*

This measure of vorticity will therefore be preserved if the pressures assigned to the edges have the property that $\mu_y P = \mu_x Q$, and this is ensured if we take $P = \mu_x r, Q = \mu_y r$, where r is some quantity defined in cells. For consistency, it should be some local mean of the pressure, and to obey the symmetry principle (section 2.2) it must be evaluated by a symmetrical operator such as $[1 + \alpha(\delta_x^2 + \delta_y^2) + \beta\delta_x^2\delta_y^2]$. The smallest possible stencil comes from taking simply $r = p$, and hence

$$P = \mu_x r = \mu_x p, \qquad Q = \mu_y r = \mu_y p,$$

which corresponds to the simplest form of central differencing used in cell-centered finite-volume schemes, for example, [2]. However, this would lead to an unconditionally unstable scheme. Averaging just in the coordinate directions, as for the well-known Lax–Friedrichs difference scheme, leads to taking $\alpha = \frac{1}{4}, \beta = 0$.

To obtain second-order accuracy P, Q should be evaluated halfway through the time step, and to preserve vorticity we need to derive them from an r that has been evaluated halfway through the time step, so that $r = p + \frac{1}{2}\Delta t \partial_t p = p - \frac{1}{2}c\Delta t \mathrm{div}\vec{u}$.

On the most compact available stencil, and maintaining stability as for the Lax–Friedrichs scheme, this leads to

$$r = [1 + \tfrac{1}{4}(\delta_x^2 + \delta_y^2)]p - \tfrac{1}{2}\nu[\mu_x\delta_x u + \mu_y\delta_y v]$$

and hence, with $P = \mu_x r, Q = \mu_y r$, (7), (8) become

$$u^{n+1} = u^n - \nu\mu_x\delta_x\{[1 + \tfrac{1}{4}(\delta_x^2 + \delta_y^2)]p - \tfrac{1}{2}\nu[\mu_x\delta_x u + \mu_y\delta_y v]\}, \tag{10}$$

$$v^{n+1} = u^n - \nu\mu_y\delta_y\{[1 + \tfrac{1}{4}(\delta_x^2 + \delta_y^2)]p - \tfrac{1}{2}\nu[\mu_x\delta_x u + \mu_y\delta_y v]\}. \tag{11}$$

If we update the pressure with the same standard central-differences, together with a four-point averaging of p to give stability, we recover Richtmyer's form of the Lax–Wendroff method, usually written as a two-step scheme [3] (see also [4, pp. 360–365]). Its vorticity-preserving property does not seem to have been previously noticed. However, in other respects, it is less desirable. The stencil is shown in Figure 2 and can be seen to involve only points of one "parity" (value of $(i + j)(\mathrm{mod}2)$). Therefore the method suffers from "odd-even decoupling." We do not consider this method further but turn to an alternative definition of discrete vorticity.

3.2. Compact vorticity. Next let us define the "compact vorticity"

$$\zeta_{\Delta_2} = \mu_y\delta_x v - \mu_x\delta_y u = Z_2\mathbf{u}. \tag{12}$$

Following the previous argument, we can preserve this if

$$\begin{aligned} 0 &= Z_2(\mathbf{u}^{n+1} - \mathbf{u}^n) \\ &= -\nu Z_2[\delta_x U + \delta_y V, \delta_x P, \delta_y Q] \\ &= \nu \delta_x \delta_y (\mu_x P - \mu_y Q), \end{aligned}$$

and the condition $\mu_x P = \mu_y Q$ will be met if we take $P = \mu_y r', Q = \mu_x r'$, where r' is some quantity defined at vertices. The only way to define a consistent local pressure while retaining a nine-point stencil is to take

$$r' = \mu_x \mu_y p. \tag{13}$$

In that case we have

$$P = \mu_x \mu_y^2 p, \qquad Q = \mu_x^2 \mu_y p. \tag{14}$$

To obtain second-order accuracy, r' must now be updated to halfway through the time step. The simple formula

$$r' = \mu_x \mu_y p - \tfrac{1}{2}\nu[\mu_y \delta_x u + \mu_x \delta_y v]$$

is the unique symmetrical formula to achieve this without enlarging the stencil, leading to

$$P = \mu_y r' = \mu_x \mu_y^2 p - \tfrac{1}{2}\nu[\mu_y^2 \delta_x u + \mu_x \mu_y \delta_y v], \tag{15}$$

$$Q = \mu_x r' = \mu_x^2 \mu_y p - \tfrac{1}{2}\nu[\mu_y \mu_x \delta_x u + \mu_x^2 \delta_y v]. \tag{16}$$

3.3. Two remarks on implementation. We insert here an important observation relating to the construction of nonlinear "limited" schemes that avoid nonphysical overshoots [5]. We do not attempt a thorough discussion of this issue in the present paper, because the objectives for such schemes are still unclear. For example, there is no maximum principle because waves may focus and increase in strength. However, we do note that any limiting applied to the intermediate quantity r' will still leave the vorticity exactly preserved. The limiter for such a scheme must, however, be centered on a vertex and therefore depend on values in the four neighboring cells. Schemes that are based, like most upwind schemes in current use, on one-dimensional reconstruction and interpolation cannot preserve vorticity in any of the above senses.

Our second remark deals with the application of boundary conditions, for example, to simulate the generation of acoustic waves by a moving boundary. In most finite-volume schemes one would derive from the boundary condition some expression for the unknown pressure at an interface (say, P, in Figure 1) in terms of the known normal velocity (say, U, for a vertical boundary). This would be incorrect. The correct procedure is to obtain vertex pressure p' in terms of given vertex velocities u'. If the condition is applied in this way one can easily show that vorticity at nodes adjacent to the wall is preserved; for any other procedure a vortical layer will be produced.

4. Construction and properties of evolution operator. We collect the results of section 3.2 into a prescription for the matrix operator that will update the solution, so that if

$$\mathbf{u}^{n+1} = \mathbf{u}^n - M_\Delta \mathbf{u}^n, \tag{17}$$

certain elements of the matrix M_Δ are already uniquely determined by insisting that the velocities are updated with second-order accuracy while preserving the discrete vorticity (12). We have in fact, from (7), (8), (15), (16),

$$M_\Delta = \begin{bmatrix} ?? & ?? & ?? \\ \nu\mu_x\mu_y^2\delta_x & \frac{1}{2}\nu^2\mu_y^2\delta_x^2 & \frac{1}{2}\nu^2\mu_x\mu_y\delta_x\delta_y \\ \nu\mu_x^2\mu_y\delta_y & \frac{1}{2}\nu^2\mu_x\mu_y\delta_x\delta_y & \frac{1}{2}\nu^2\mu_x^2\delta_y^2 \end{bmatrix}.$$

The adjoint property $\mathrm{div}_h = -\mathrm{grad}_h^*$ requires that this matrix be symmetric, hence

$$M_\Delta = \begin{bmatrix} ?? & \nu\mu_x\mu_y^2\delta_x & \nu\mu_x^2\mu_y\delta_y \\ \nu\mu_x\mu_y^2\delta_x & \frac{1}{2}\nu^2\mu_y^2\delta_x^2 & \frac{1}{2}\nu^2\mu_x\mu_y\delta_x\delta_y \\ \nu\mu_x^2\mu_y\delta_y & \frac{1}{2}\nu^2\mu_x\mu_y\delta_x\delta_y & \frac{1}{2}\nu^2\mu_x^2\delta_y^2 \end{bmatrix}$$

and only the $1,1$ element remains open. This can be determined by noting that the flux U, say, is implied by the above formula to be

$$U = \mu_x\mu_y^2 u = \mu_y(\mu_x\mu_y u) = \mu_y u',$$

where $u' = \mu_x\mu_y u$ is an average evaluated at the vertices, as in (13). To update this to $(n+\frac{1}{2})\Delta t$ we need to add a term $-\frac{1}{2}\Delta t\partial_x p$ which can only be $-\frac{1}{2}\nu\mu_y\delta_x p$. By considering V also, we finally arrive at

$$M_\Delta = \begin{bmatrix} \frac{1}{2}\nu^2(\mu_y^2\delta_x^2 + \mu_x^2\delta_y^2) & \nu\mu_x\mu_y^2\delta_x & \nu\mu_x^2\mu_y\delta_y \\ \nu\mu_x\mu_y^2\delta_x & \frac{1}{2}\nu^2\mu_y^2\delta_x^2 & \frac{1}{2}\nu^2\mu_x\mu_y\delta_x\delta_y \\ \nu\mu_x^2\mu_y\delta_y & \frac{1}{2}\nu^2\mu_x\mu_y\delta_x\delta_y & \frac{1}{2}\nu^2\mu_x^2\delta_y^2 \end{bmatrix}. \tag{18}$$

The scheme represented by this matrix has been uniquely determined by the requirements of conservation, vorticity preservation, symmetry of the solution under grid transformations, adjoint symmetry of the discrete operator, and second-order accuracy. Again, however, it is not a new scheme. It can be recognized by noting that M_Δ can be factored as

$$M_\Delta = \nu L_\Delta[\mu_x\mu_y I - \tfrac{1}{2}\nu L_\Delta], \tag{19}$$

where

$$L_\Delta = \begin{bmatrix} 0 & \mu_y\delta_x & \mu_x\delta_y \\ \mu_y\delta_x & 0 & 0 \\ \mu_x\delta_y & 0 & 0 \end{bmatrix}, \tag{20}$$

and therefore can be written as a two-step scheme. The operation

$$\mathbf{u}' = [\mu_x\mu_y I - \tfrac{1}{2}\nu L_\Delta]\mathbf{u}^n \tag{21}$$

gives a provisional solution at the vertices. The operation

$$\mathbf{u}^{n+1} = \mathbf{u}^n - \nu L_\Delta \mathbf{u}' \tag{22}$$

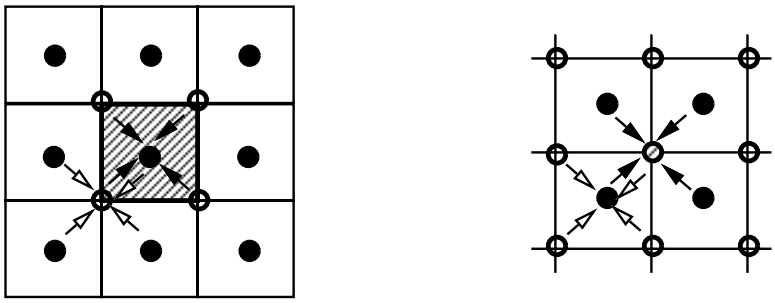

FIG. 3. *(left) The rotated Richtmyer scheme. In the first step, symbolized by white arrows, data from the cells are used to create a half time-step solution at the vertices. In the second step (black arrows) integration round the vertices updates the central cell. (right) Ni's cell-vertex scheme. In the first step (white arrows) we integrate around the cells to obtain a "cell-residual." In the second step (black arrows) these are distributed to the vertices.*

completes the update by integrating around the vertices. This is in fact the version of Lax–Wendroff known as the rotated Richtmyer scheme (see, e.g., [5, p. 125]). It is shown schematically on the left of Figure 3; comparing with Figure 2 we see the reason for the name. The original motivations for this scheme were compactness, computational economy, and stability. In the nonlinear case, as in all two-step Lax–Wendroff schemes, one avoids any multiplication by the Jacobian matrices. The vorticity-preserving property does not seem to have been previously noticed.

The second step of the method is of course a leapfrog scheme. Usually the dissipative first step is desirable to enhance stability, especially in the nonlinear case. However, we could, if we wished, construct the "pure" leapfrog method,

$$\mathbf{u}^{n+1} = \mathbf{u}^{n-1} - 2\nu L_\Delta \mathbf{u}^n, \tag{23}$$

and it is clear that this scheme would also be vorticity-preserving. So indeed would a multistage method of Runge–Kutta type [2] in which each stage employed the operator L_Δ.

4.1. Duality. Since both factors of M_Δ depend only on L_Δ they commute, and so the scheme may also be written as

$$\mathbf{u}^{n+1} - \mathbf{u}^n = -\nu[\mu_x\mu_y I - \tfrac{1}{2}\nu L_\Delta]L_\Delta \mathbf{u}^n. \tag{24}$$

In this form it is Ni's cell-vertex scheme [7], in which the variables are usually thought of as located at vertices of a grid, defining a bilinear interpolant over a square element. The first step L_Δ is to integrate $\partial_x\mathbf{F} + \partial_y\mathbf{G}$ over this element and the second step is to distribute this to the nodes of the element. It is easy to check that if some cell variable q is distributed to the nodes in the four ways shown in Figure 4, the updates to the vertices are, respectively,

$$\mu_x\mu_y q, \qquad \mu_y\delta_x q, \qquad \mu_x\delta_y q, \qquad \delta_x\delta_y q.$$

Ni's scheme was devised in the context of solving steady-state aerodynamic problems. If the transients are not required to be accurately resolved, one may consider variants of the form

$$\mathbf{u}^{n+1} - \mathbf{u}^n = -\nu[\mu_x\mu_y I - \tfrac{1}{2}\nu' L'_\Delta]L_\Delta \mathbf{u}^n,$$

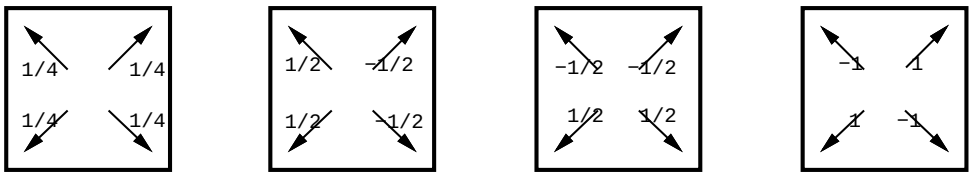

FIG. 4. *Distribution strategies.*

where ν' and L'_Δ may not be the same as ν and L_Δ. Such a scheme will not in general preserve vorticity.

However, vorticity is preserved by those schemes in which $L'_\Delta = L_\Delta$; smoother solutions are obtained by taking ν small and ν' large such that $\nu\nu' \leq 1$ (see [8] and the next section).

4.2. Energy conservation and stability. At the PDE level, we have in two dimensions the classical energy invariance

$$\begin{aligned}\frac{d}{dt}\iint \tfrac{1}{2}(p^2+u^2+v^2)dxdy &= \iint (p\partial_t p + u\partial_t u + v\partial_t v)dxdy \\ &= -\langle p, \mathrm{div}(u,v)\rangle - \langle (u,v)^T, \mathrm{grad} p\rangle \\ &= -\langle 1, \mathrm{div}(pu,pv)\rangle \\ &= 0.\end{aligned}$$

This proof turns on the relationship $\mathrm{div} = -\mathrm{grad}^*$, where $()^*$ denotes the adjoint operator.

To obtain stability in the discrete case we will require analogous discrete properties. In fact, the choices for $\mathbf{F}^*, \mathbf{G}^*$ derived above utilize discrete definitions $(\mathrm{div})_h$ and $(\mathrm{grad})_h$ which actually possess an adjoint relationship through the summation-by-parts formulae in section 2.1. In the following section we use this fact to prove energy stability of the scheme.

5. Stability and truncation error.

5.1. Stability. In this section, we consider a slight generalization of the update operator, taking

$$M_\Delta = \nu\mu_x\mu_y L_\Delta - \tfrac{1}{2}qL_\Delta^2, \tag{25}$$

where q is a parameter controlling the numerical dissipation. All schemes of this family preserve vorticity in the sense of section 3.2. In general they are first-order accurate unless $q = \nu^2$. Denoting Fourier transforms of $\mathbf{u}, M_\Delta, L_\Delta$ by $\widehat{\mathbf{u}}, \widehat{M}_\Delta, \widehat{L}_\Delta$ we write the stability condition as

$$\widehat{\mathbf{u}}^*[I - \widehat{M}_\Delta^*][I - \widehat{M}_\Delta]\widehat{\mathbf{u}} \leq \widehat{\mathbf{u}}^*\widehat{\mathbf{u}},$$

where $()^*$ denotes the Hermitian operator. We write

$$\widehat{L}_\Delta = 2\mathrm{i}\begin{bmatrix} 0 & \alpha & \beta \\ \alpha & 0 & 0 \\ \beta & 0 & 0 \end{bmatrix},$$

where $\alpha = \cos(\frac{1}{2}k_y h)\sin(\frac{1}{2}k_x h), \beta = \cos(\frac{1}{2}k_x h)\sin(\frac{1}{2}k_y h)$, and k_x, k_y are the wave numbers; note that $\widehat{L}^*_\Delta = -\widehat{L}_\Delta$. Then, abbreviating also $c_x = \cos(\frac{1}{2}k_x h), c_y = \cos(\frac{1}{2}k_y h)$ so that $\hat{\mu}_x\hat{\mu}_y = c_x c_y$, we have

$$\begin{aligned}[I - \widehat{M}^*_\Delta][I - \widehat{M}_\Delta] &= [I + \nu c_x c_y \widehat{L}_\Delta + \tfrac{1}{2}q\widehat{L}^2_\Delta][I - \nu c_x c_y \widehat{L}_\Delta + \tfrac{1}{2}q\widehat{L}^2_\Delta] \\ &= [I + (q - \nu^2 c_x^2 c_y^2)\widehat{L}^2_\Delta + \tfrac{1}{4}q^2\widehat{L}^4_\Delta].\end{aligned}$$

After carrying out the multiplications, we have

$$\widehat{\mathbf{u}}^*[I - \widehat{M}^*_\Delta][I - \widehat{M}_\Delta]\widehat{\mathbf{u}} = \|\widehat{\mathbf{u}}\|^2 - 4[(q - \nu^2 c_x^2 c_y^2) - q^2(\alpha^2 + \beta^2)][(\alpha^2 + \beta^2)|\hat{p}|^2 + |\alpha\hat{u} + \beta\hat{v}|^2]$$

so that the stability condition is

$$(\alpha^2 + \beta^2)q^2 \le q - \nu^2 c_x^2 c_y^2 \tag{26}$$

for all modes.

LEMMA 1. *The scheme is stable if*

$$\nu^2 \le q \le 1. \tag{27}$$

Proof. Necessity of the left inequality follows from considering $k_x = k_y = 0$, and necessity of the right inequality from $k_x h = \pi, k_y = 0$. Sufficiency follows from noting

$$\alpha^2 + \beta^2 = 1 - (1 - c_x^2)(1 - c_y^2) - c_x^2 c_y^2 \le 1 - c_x^2 c_y^2$$

so that

$$\begin{aligned}(\alpha^2 + \beta^2)q^2 - q + \nu^2 c_x^2 c_y^2 &\le (1 - c_x^2 c_y^2)q^2 - q + \nu^2 c_x^2 c_y^2 \\ &= (\nu^2 - q)c_x^2 c_y^2 + q(q-1)(1 - c_x^2 c_y^2) \le 0. \qquad \square\end{aligned}$$

As well as the special choice $q = \nu^2$ leading to the second-order scheme, one may note other stable choices. Taking $q = 1$ gives a Lax–Friedrichs scheme, and $q = \nu$ gives a scheme that reduces to the first-order upwind scheme if the data is one-dimensional. It may be conjectured that this latter scheme will have an important role to play in the development of nonlinear, "limited" methods. Finally, the parameter q may be identified with the product $\nu\nu'$ mentioned in the previous section.

In the appendix we use Fourier analysis to estimate the rate of vorticity production by comparable schemes which have not been designed to preserve it. In particular, an expression is given for the vorticity production by the standard one-step Lax–Wendroff method.

5.2. Truncation error. The amplification factor that results from applying the operator L_Δ to an arbitrary Fourier mode is, using the above notation, $2\mathrm{i}\sqrt{\alpha^2 + \beta^2}$ and hence the amplification factor of the operator $1 - M_\Delta$ is, for $q = \nu^2$,

$$g = 1 - 2\mathrm{i}\nu\hat{\mu}_x\hat{\mu}_y\sqrt{\alpha^2 + \beta^2} - 2\nu^2(\alpha^2 + \beta^2).$$

This has a modulus given by

$$|g|^2 = 1 - 4\nu^2(1 - c_x^2 c_y^2)(\alpha^2 + \beta^2) + 4\nu^4(\alpha^2 + \beta^2)^2.$$

Expanding this as a Taylor series in k_x, k_y leads to

$$|g| = 1 - \frac{h^4}{8}\nu^2(1 - \nu^2)(k_x^2 + k_y^2)^2 + \mathcal{O}(h^6), \tag{28}$$

which is isotropic to leading order. The amplification error over a number of time steps proportional to h^{-1} (that is, over some fixed time independent of the grid) is $\mathcal{O}(h^3)$.

The phase error is given by the ratio of numerical to exact propagation speeds

$$\frac{\arg g}{\frac{1}{2}\sqrt{k_x^2+k_y^2}h} = 1 - \frac{h^2}{8}(1-\nu^2)(k_x^2+k_y^2) - \frac{h^2}{24}\frac{k_x^2k_y^2}{k_x^2+k_y^2} + \mathcal{O}(h^4), \tag{29}$$

which is $\mathcal{O}(h^2)$ and is not isotropic.

6. Including advection. If the linearization is not with respect to a stationary flow but with respect to a uniform flow with velocity (u_0, v_0), the differential operator becomes

$$L^Q = \frac{1}{c}\begin{bmatrix} u_0\partial_x + v_0\partial_y & c\partial_x & c\partial_y \\ c\partial_x & u_0\partial_x + v_0\partial_y & 0 \\ c\partial_y & 0 & u_0\partial_x + v_0\partial_y \end{bmatrix}, \tag{30}$$

from which we may easily deduce that vorticity is a convected quantity,

$$(\partial_t + u_0\partial_x + v_0\partial_y)(\partial_x v - \partial_y u) = 0. \tag{31}$$

6.1. Discrete vorticity advection. This is very simply achieved. Define

$$L_\Delta^Q = \begin{bmatrix} Q_\Delta & \mu_y\delta_x & \mu_x\delta_y \\ \mu_y\delta_x & Q_\Delta & 0 \\ \mu_x\delta_y & 0 & Q_\Delta \end{bmatrix}, \tag{32}$$

where Q_Δ is any discrete operator consistent with $(u_0\partial_x + v_0\partial_y)/c$ that maps between the cell center and cell vertex meshes. Then the evolution of vorticity ζ_{Δ_2} under a first-order application of this operator is given by

$$\begin{aligned} \zeta_{\Delta_2}^{n+1} - \zeta_{\Delta_2}^n &= Z_2\mathbf{u}^{n+1} - Z_2\mathbf{u}^n \\ &= -\nu Z_2[Q_\Delta I + L_\Delta]\mathbf{u}' \\ &= -\nu Z_2 Q_\Delta \mathbf{u}' \\ &= -\nu Q_\Delta Z_2 \mathbf{u}' \\ &= -\nu Q_\Delta \zeta'_{\Delta_2}. \end{aligned} \tag{33}$$

A Lax–Wendroff scheme defined by

$$\mathbf{u}^{n+1} - \mathbf{u}^n = -\nu L_\Delta^Q[\mu_x\mu_y I - \tfrac{1}{2}\nu L_\Delta^Q]\mathbf{u}^n$$

will lead to

$$\zeta_{\Delta_2}^{n+1} - \zeta_{\Delta_2}^n = -\nu Q_\Delta[\mu_x\mu_y I - \tfrac{1}{2}\nu Q_\Delta]\zeta_{\Delta_2}^n, \tag{34}$$

so that ζ_{Δ_2} is transported by the Lax–Wendroff version of Q_Δ.

6.2. Stability with advection. For consistency in our choice of difference operators we will take Q_Δ above to be

$$Q_\Delta = \frac{1}{c}(u_0\mu_y\delta_x + v_0\mu_x\delta_y) \tag{35}$$

so that the Fourier symbol of the update operator becomes

$$\widehat{L}^Q_\Delta = 2\mathrm{i}\begin{bmatrix} \gamma & \alpha & \beta \\ \alpha & \gamma & 0 \\ \beta & 0 & \gamma \end{bmatrix}, \tag{36}$$

where $\gamma = M_x\alpha + M_y\beta$ and $M_x = u_0/c, M_y = u_0/c$ are Mach numbers of the undisturbed flow in the (x, y)-directions.

In this section we use an alternative analysis in terms of the eigenvalues of the evolution operator, exploiting the fact that only powers of the first-order operator are involved. Suppose that $\widehat{L}^Q_\Delta$ has an eigenvalue $2\mathrm{i}\kappa$. Then the Fourier symbol of the second-order update operator

$$I - \nu\mu_x\mu_y L^Q_\Delta + \tfrac{1}{2}q(L^Q_\Delta)^2$$

has an eigenvalue

$$1 - 2\mathrm{i}\nu\hat{\mu}_x\hat{\mu}_y\kappa - 2q\kappa^2,$$

and this has modulus less than unity if

$$\kappa^2 q^2 \le q - \nu^2 c_x^2 c_y^2. \tag{37}$$

Now, κ is actually equal to either γ or $\gamma \pm \sqrt{\alpha^2 + \beta^2}$ so that in either case

$$\kappa^2 \le \gamma^2 + 2|\gamma|\sqrt{\alpha^2 + \beta^2} + \alpha^2 + \beta^2.$$

Using the fact that $|\gamma| \le |M|\sqrt{\alpha^2 + \beta^2}$ we obtain

$$\kappa^2 \le (|M| + 1)^2(\alpha^2 + \beta^2)$$

so that from (37) the stability condition becomes

$$(1 + |M|)^2(\alpha^2 + \beta^2)q^2 \le q - \nu^2 c_x^2 c_y^2 \tag{38}$$

for all modes, which may be compared with (26). From the analysis of that equation it follows that the necessary and sufficient condition for stability of all modes in the presence of advection is

$$\nu^2 \le q \le \left(\frac{1}{1 + |M|}\right)^2. \tag{39}$$

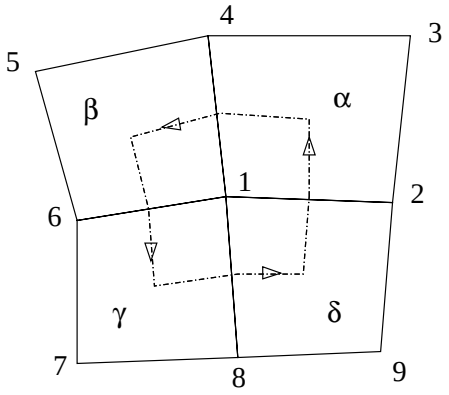

FIG. 5. *Cell and vertex numbering for a quadrilateral mesh.*

7. Irregular grids. We now turn our attention to irregular grids. Our aim is to find some measure of vorticity that is exactly preserved. More significantly, if that measure can be expressed as a line integral around some small control volume, and if many such control volumes can be united to make a large control volume, there will be a global conservation principle for circulation.

This is where the two interpretations of our scheme diverge. In the cell-centered finite-volume approach the velocities are piecewise constant within each cell so that circulation will be evaluated by a rectangle rule. In a vertex-centered finite-difference interpretation, velocities vary bilinearly within each element so that circulation will be evaluated by a trapezium rule. Even on a re-entrant path on a square grid these are equivalent so that both interpretations lead to a circulation-preserving scheme. On irregular grids the measures of circulation are different and it is not obvious that any correspondence exists.

In fact, we have only been able to prove preservation of circulation for the cell-centered finite-volume scheme, and have come to suspect rather strongly that there is no such result for the vertex-centered finite-difference method.

7.1. Quadrilateral cells. Suppose the square cells of Figure 1 are distorted to give the quadrilaterals of Figure 5, and the solution is updated by a two-step scheme as in (21), (22) with the intermediate quantities $\mathbf{u}'$ held at the vertices of the quadrilaterals. To calculate the update we suppose that $\mathbf{u}'$ is bilinearly interpolated over each quadrilateral from the vertex values. Then we show that a natural generalization of the discrete vorticity $Z_2\mathbf{u}$ is exactly preserved.

With the cell and vertex numbering of Figure 5, the update to the cell average $\mathbf{u}_\alpha$ is obtained by integrating $L\mathbf{u}'$ over the quadrilateral Ω_α of measure V_α and by applying Gauss's theorem to obtain a line integral around the perimeter of the cell. Thus for u we obtain

$$u_\alpha^{n+1} - u_\alpha^n = -\frac{c\Delta t}{V_\alpha}\int_{\Omega_\alpha} \partial_x p' d\Omega = -\frac{c\Delta t}{V_\alpha}\oint_{\partial\Omega_\alpha} p' dy$$

$$= -\frac{c\Delta t}{2V_\alpha}[(p'_1 - p'_3)(y_2 - y_4) + (p'_2 - p'_4)(y_3 - y_1)], \tag{40}$$

where the integrals along each edge are given exactly by use of the trapezoidal rule. Similarly for v we obtain

$$v_\alpha^{n+1} - v_\alpha^n = -\frac{c\Delta t}{V_\alpha}\int_{\Omega_\alpha} \partial_y p' d\Omega = \frac{c\Delta t}{V_\alpha}\oint_{\partial\Omega_\alpha} p' dx$$
$$= \frac{c\Delta t}{2V_\alpha}[(p'_1 - p'_3)(x_2 - x_4) + (p'_2 - p'_4)(x_3 - x_1)]. \tag{41}$$

The change in discrete vorticity at vertex 1 is then obtained by integrating the change in $\partial_x v - \partial_y u$ over an appropriate region and again turning this into a line integral of the form

$$\Delta\Gamma = \oint [(v^{n+1} - v^n)dy + (u^{n+1} - u^n)dx], \tag{42}$$

where (u, v) are constant in each quadrilateral and the line integral represents the circulation. Preservation of vorticity can be ensured by appropriately choosing a path for the line integral. We choose the part of the line in cell Ω_α to run from the midpoint of the side $(1, 2)$ to the centroid and then to the midpoint of side $(1, 4)$. In fact, since (u, v) are constant along this path, the integral is the same for any path joining the midpoints of the sides, but making it go through the centroid ensures that the control volumes can be joined together. The contribution to (42) at vertex 1 from (40) and (41) is then, after some crucial cancellation,

$$\Delta\Gamma_{1,\alpha} = \tfrac{1}{2}[(v_\alpha^{n+1} - v_\alpha^n)(y_4 - y_2) + (u_\alpha^{n+1} - u_\alpha^n)(x_4 - x_2)]$$
$$= \frac{c\Delta t}{4V_\alpha}(p'_2 - p'_4)[(y_4 - y_2)(x_3 - x_1) - (x_4 - x_2)(y_3 - y_1)]$$
$$= \tfrac{1}{2}c\Delta t(p'_2 - p'_4), \tag{43}$$

because the quantity in square brackets on the line above (43) is just $2V_\alpha$. It is now clear that as we add the contributions from cells $\Omega_\alpha, \Omega_\beta, \Omega_\gamma$, and Ω_δ, which meet at the vertex 1, they all cancel. Thus there is no change in the circulation around the contour chosen, and so the discrete vorticity defined by (42) and (43) is exactly preserved.

7.2. Mixed meshes. Suppose we have a mesh in which any combination of triangles and quadrilaterals meets at every vertex. Again we define the vorticity at that vertex through (42). Then, with the numbering of Figure 6, the line integrals for the update in triangular cell Ω_α can be computed as in (40), (41) to give

$$\begin{pmatrix} u \\ v \end{pmatrix}_\alpha^{n+1} - \begin{pmatrix} u \\ v \end{pmatrix}_\alpha^{n} = -\frac{c\Delta t}{2V_\alpha}\left[p'_1\begin{pmatrix} y_2 - y_3 \\ x_3 - x_2 \end{pmatrix} + p'_2\begin{pmatrix} y_3 - y_1 \\ x_1 - x_3 \end{pmatrix} + p'_3\begin{pmatrix} y_1 - y_2 \\ x_2 - x_1 \end{pmatrix}\right]$$
$$= \frac{c\Delta t}{2V_\alpha}\left[(p'_2 - p'_1)\begin{pmatrix} y_1 - y_3 \\ x_3 - x_1 \end{pmatrix} + (p'_3 - p'_1)\begin{pmatrix} y_2 - y_1 \\ x_1 - x_2 \end{pmatrix}\right]. \tag{44}$$

It is also clear that the area of the triangle is given by

$$V_\alpha = \tfrac{1}{2}[x_1(y_2 - y_3) + x_2(y_3 - y_1) + x_3(y_1 - y_2)]$$
$$= -\tfrac{1}{2}[y_1(x_2 - x_3) + y_2(x_3 - x_1) + y_3(x_1 - x_2)]. \tag{45}$$

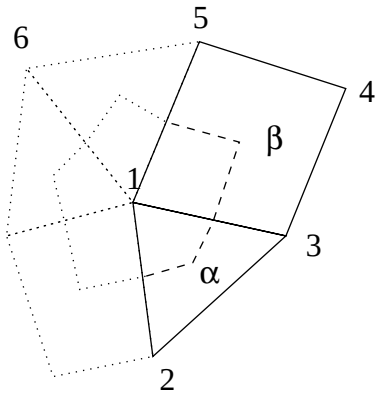

FIG. 6. *Cell and vertex numbering for a mixed mesh.*

Hence the vorticity change computed from all the triangular cells meeting at vertex 1 is in the form of a line integral,

$$\begin{aligned}&\oint[(v^{n+1}-v^n)dy+(u^{n+1}-u^n)dx]\\ &\quad=c\Delta t\sum_{(\alpha)}\frac{1}{2V_\alpha}[(v_\alpha^{n+1}-v_\alpha^n)\Delta y_\alpha+(u_\alpha^{n+1}-u_\alpha^n)\Delta x_\alpha],\end{aligned}\tag{46}$$

into which the u and v updates are substituted from (44).

As in the quadrilateral case, we choose the line integrals to go from the midpoints of edges to the centroids of each triangle. Thus in cell Ω_α we have $\Delta x_\alpha = \frac{1}{2}(x_3 + x_1) - \frac{1}{2}(x_2 + x_1) = \frac{1}{2}(x_3 - x_2)$. As a result, the contribution from Ω_α to the update of circulation around vertex 1 may be written

$$\begin{aligned}\Delta\Gamma_{1,\alpha}&=\frac{c\Delta t}{4V_\alpha}\left[\{(p_2'-p_1')(y_3-y_1)+(p_3'-p_1')(y_1-y_2)\}(x_3-x_2)\right.\\ &\qquad\left.+\{(p_2'-p_1')(x_1-x_3)+(p_3'-p_1')(x_2-x_1)\}(y_3-y_2)\right]\\ &=\frac{c\Delta t}{4V_\alpha}\left[p_2'\{(y_3-y_1)(x_3-x_2)+(x_1-x_3)(y_3-y_2)\}\right.\\ &\qquad\left.+p_3'\{(y_1-y_2)(x_3-x_2)+(x_2-x_1)(y_3-y_2)\}\right]\\ &=\frac{c\Delta t}{2}(p_2'-p_3').\end{aligned}\tag{47}$$

Since this is of exactly the same form as (43) the total update to the circulation around vertex 1 vanishes, and since the control volumes for any set of contiguous vertices can be merged into one large control volume as in Figure 7, the circulation around that remains unchanged also.

If cells with more than four vertices are considered, their contribution involves the values of p' at vertices that are not common to two cells and which therefore do not cancel. It seems that meshes made from a mixture of quadrilaterals and triangles are the most general for which this particular result holds.

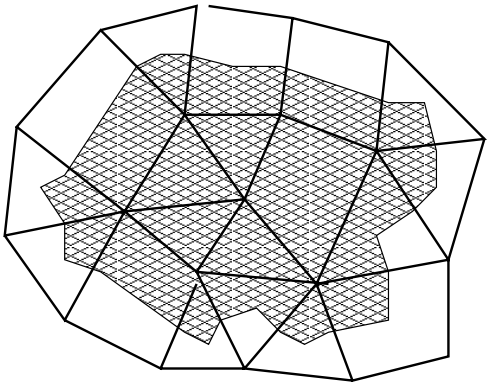

FIG. 7. *Contour for defining circulation.*

7.3. Three-dimensional unstructured grids. In three dimensions the circulation around some closed surface is the vectorial quantity

$$\vec{\Gamma} = \int\int \vec{u} \times d\vec{n}, \tag{48}$$

which evolves, for the three-dimensional version of (1), according to

$$\partial_t \vec{\Gamma} = -\int\int c\, \nabla p \times d\vec{n}, \tag{49}$$

and this vanishes if c is constant.

For finite-volume schemes, it is possible to show that a discrete version of (48) remains invariant for grids that are arbitrary combinations of tetrahedra and hexahedra if a suitable control volume is chosen around each vertex. This is constructed as shown in Figure 8 . For tetrahedral cells, one constructs the six planes defined by one edge and the midpoint of the opposite edge, thereby dissecting the tetrahedron into four hexahedra, one associated with each vertex. For hexahedral cells, one creates eight small hexahedra by constructing the three bilinear surfaces that bisect pairs of

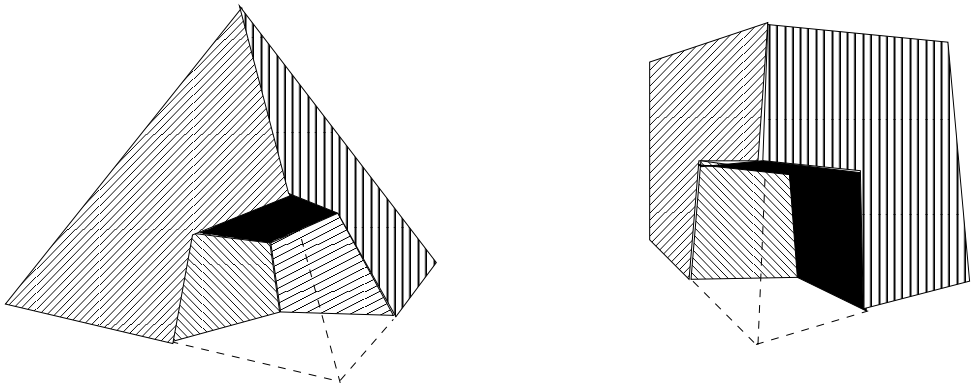

FIG. 8. *Elements of a mixed three-dimensional unstructured grid, showing a tetrahedral cell (left) and a hexahedral cell (right) with the subvolume corresponding to one vertex cut away.*

opposite faces. The control volume around any given vertex is the union of subcells so constructed. An appropriate measure for the circulation around this control volume is

$$\vec{\Gamma}_V = \sum \vec{u}_{\text{cell}} \vec{n}_{\text{cell}}, \tag{50}$$

where the sum is over all cells meeting at V, $\vec{u}_{\text{cell}}$ is the constant velocity associated with that cell, and $\vec{n}_{\text{cell}}$ is the "integrated normal" $\int\int \vec{n} dS$ over the boundary between the subvolume of the cell associated with V and the remainder of the cell. (Recall that $\vec{n}_{\text{cell}}$ depends only on the perimeter of that boundary and not on the surface spanning it; we choose a particular surface only to ensure that the control volumes fill the whole space.) We now sketch a proof that this circulation remains constant.

After some rather lengthy algebra, the contribution made by some cell α to the circulation around V can be written as a sum over a certain set of edges. Think of the cells meeting at V as defining some irregular polyhedron. The edges of this polyhedron that divide α from its neighbors may be called the boundary of α with respect to V and for the kind of grid considered will be either a triangle or a (probably nonplanar) hexahedron. Suppose that it is a hexahedron whose vertices have position vectors $\mathbf{r}_1, \mathbf{r}_2, \mathbf{r}_3, \mathbf{r}_4, \mathbf{r}_5, \mathbf{r}_6$. The relationship is

$$\Delta\vec{\Gamma}_{V,\alpha} = \frac{c\Delta t}{4} \sum_{j=1}^{j=6} (p_j + p_{j+1})(\mathbf{r}_{j+1} - \mathbf{r}_j). \tag{51}$$

From this equation it is clear that if c is a constant, the sum over the boundaries of all cells surrounding V will vanish, because every edge appears twice with opposite sign. If c is not a constant, then the sum becomes a consistent discretization of $-\int\int c\nabla p \times \vec{n}_{\text{cell}}$, and hence the circulation around any assembly of these control volumes depends only on a surface summation. Noting that the formulae remain valid when the hexahedra are degenerate, in particular when they degenerate to tetrahedra, completes the outline of the proof.

8. Variable coefficients. As an example of how the techniques of the present paper may be extended to problems with variable coefficients, we consider the case of acoustic waves in a fluid of variable density ρ. Then the system (1) is replaced by

$$\partial_t p + \rho a^2(\partial_x u + \partial_y v) = 0, \;\; \partial_t u + (1/\rho)\partial_x p = 0, \;\; \partial_t v + (1/\rho)\partial_y p = 0, \tag{52}$$

and the change in vorticity, $\zeta = \partial_x v - \partial_y u$, is given by

$$\begin{aligned} \partial_t \zeta &= -\partial_x(1/\rho)\partial_y p + \partial_y(1/\rho)\partial_x p \\ &= [\rho_x p_y - \rho_y p_x]/\rho^2. \end{aligned} \tag{53}$$

This represents the barotropic effect through which an inviscid flow may acquire vorticity, unless the pressure and density gradients are parallel. The integral version of this effect is Kelvin's theorem,

$$\partial_t \Gamma = \oint \frac{dp}{\rho}, \tag{54}$$

where $\Gamma = \oint \vec{u} \cdot \vec{ds}$ is the circulation around some given contour.

Now let us consider the update of the velocities on the quadrilateral mesh of Figure 5 with an appropriate modification of (40) and (41). In fact, let us take R_α as

the constant value of $1/\rho$ in cell Ω_α so that these update formulae need to be modified only by a factor R_α. The resulting change in the discrete vorticity $Z_2\mathbf{u}$ at vertex 1 is given by replacing c by R_α in (43) and summing over the cells. The result is

$$\begin{aligned} Z_2(\mathbf{u}^{n+1} - \mathbf{u}^n) = \tfrac{1}{2}\Delta t[&R_\alpha(p'_2 - p'_4) + R_\beta(p'_4 - p'_6) \\ &+R_\gamma(p'_6 - p'_8) + R_\delta(p'_8 - p'_2)]. \end{aligned} \tag{55}$$

Moreover, it is clear that the same argument applies on the mixed grid of Figure 6, and that if we merge any set of contiguous control volumes as in Figure 7, then a discrete version of Kelvin's theorem applies to such circuits of arbitrary size.

To relate this to the local formula (53), we note that (55) can be rearranged to give

$$\begin{aligned} \tfrac{1}{4}\Delta t\{&(R_\alpha - R_\gamma)[(p'_2 - p'_4) + (p'_8 - p'_6)] + (R_\beta - R_\delta)[(p'_4 - p'_6) + (p'_2 - p'_8)] \\ &+ (R_\alpha - R_\beta + R_\gamma - R_\delta)(p'_2 - p'_4 + p'_6 - p'_8)\}. \end{aligned} \tag{56}$$

Now if the mesh in Figure 5 is roughly rectangular, $R_\alpha - R_\gamma$ is a difference of R in the NW direction while $(p'_2 - p'_4) + (p'_8 - p'_6)$ is an averaged difference of p' in the roughly orthogonal NE direction; and $R_\delta - R_\beta$ is a difference of R in the NE direction while $(p'_4 - p'_6) + (p'_2 - p'_8)$ is an averaged difference of p' in the NW direction. Thus the first line of (56) will be close to zero when the gradients of R and p' are parallel, matching the behavior of (53). The second line of (56) is a product of crossed second derivatives of R and p' and will normally be two orders smaller.

This example demonstrates how properties of vorticity preservation in the differential system, even those that hold in the presence of variable coefficients, can still be reflected in our discrete schemes. With appropriate control volumes they still hold for three-dimensional unstructured grids, as in section 7.3. The case of variable coefficients in Maxwell's equations is actually easier, because the coefficients appear inside the derivative, meaning that the magnetic field remains curl-free in an arbitrary nonresistive medium. Our method will mimic this precisely.

9. Concluding discussion. A great step forward in CFD was the casting of discrete representations into conservation form by Lax and Wendroff [9]. This ensured that any shock waves captured by the scheme would be in some sense "correct" and greatly extended the range of application of numerical methods. Conservation of derived quantities seems to have received much less attention since the early work of Arakawa [10] and Jesperson [11] on schemes that conserve total energy and enstrophy. In particular, there seems to have been little exploration of the conservation of local derivative quantities such as vorticity which is the object of study in this paper.

By starting with the simplest case of linear problems on square grids treated by Lax–Wendroff methods, we have been able to reduce the number of candidate schemes. In fact, insisting on conservation of the primary quantities and the derivatives, together with symmetry and compactness properties, makes the scheme essentially unique. We have analyzed the stability of the scheme and find that either with or without advective terms it is stable up to the largest time steps that the CFL condition allows.

Expressing the update operator as the product of two commuting factors allows just two interpretations, depending on the order of their execution. One interpretation is as a cell-centered finite-volume scheme, whereas the other is as a vertex-centered finite-difference scheme. On irregular grids the operators no longer commute, and the two interpretations are different. We show that the finite-volume interpretation

continues to preserve vorticity, but it is a finite-volume scheme of a somewhat nontraditional kind. There is a unique flux through each interface, but it may not be evaluated by reference only to the pair of cells that it separates; it must be found by averaging the fluxes at its two end points and therefore involves four cell states. Apparently this is the price to be paid for incorporating the additional conservation properties.

Whether this price will buy worthwhile benefits remains to be seen. In [12] a number of alternative nine-point schemes are given, some of which have attractive properties, but they are not vorticity-preserving. These schemes are designed by approximating the exact evolution operator for the PDE (using the bicharacteristics of the wave equation in this case) and then projecting onto piecewise constant functions. Unfortunately these approximations to the evolution operator destroy the vorticity preservation. On the other hand the schemes generated in the present paper can be regarded as evolution Galerkin methods in which Taylor expansions in time are used to approximate the evolution operator; this has the advantage of preserving vorticity. For the schemes in [12] the changes in vorticity can be estimated and shown to be quite substantial relative to other truncation error terms. Vorticity production by a general class of schemes, which includes the standard one-step Lax–Wendroff method, is presented briefly in the appendix.

Moreover, there is one rather substantial practical problem to which the current approach might be relevant. This is the appearance in many shock-capturing codes of anomalous solutions, such as the "carbuncle" that often appears ahead of blunt bodies in supersonic flow computations, first reported in [13] and recently investigated thoroughly in [14]. Closely related to this is "Quirk's phenomenon" [15] that produces an odd-even decoupling in response to small mesh perturbations, and the kinks that sometimes appear in reflected Mach stems [15, 16]. It seems very probable that these are truly weak solutions, even entropy-satisfying weak solutions, of the Euler equations, even though not usually observed in practice.[1]

Very often, perhaps always, these anomalous solutions are marked by the presence of nonphysical vorticity; in the carbuncle this accumulates into two massive counter-rotating vortices. Robinet et al. [17] note a marked correspondence between the Quirk phenomenon and a previously overlooked form of shock instability involving resonance between vortical and acoustic modes. It is therefore a reasonable speculation that a method based to some extent on the control of vorticity might be less prone to producing anomalous solutions, and might even avoid them altogether. At the moment they are usually eliminated by adding numerical dissipation in a somewhat indiscriminate manner.

But as stated earlier, we regard the present paper merely as a beginning and hope to present various extensions, both theoretical and practical, in future publications. Some extensions are very easy, such as the consideration of Maxwell's equations or ideal MHD, where the differential constraint involves the divergence rather than the curl. We have begun to consider higher-order extensions and consistent finite-element versions. We have not yet seriously thought about fully nonlinear problems or moving meshes, both of which are necessary steps to take if these ideas are indeed to have

[1]The carbuncle phenomenon can be created in a wind tunnel. One inserts a thin splitter-plate ahead of the tip of the body. A Schlieren photograph of the resulting flow appears as Plate 272 in [18]. Quite possibly the vorticity created by the boundary layer on the plate is responsible, but the high Reynolds number limit of this flow is a valid solution of the Euler equations. We conjecture that anomalous Euler solutions result from the systematic creation of vorticity due to truncation error.

practical impact on complex problems. Neither have we ourselves yet conducted any numerical experiments, although we plan on doing so soon. In the meantime we are grateful to Professor Alain Lerat who has had some experiments carried out in his laboratory when the second author was visiting there [21]: these confirm the predictions of the analysis. For initial data representing a stationary vortex they show substantial vorticity losses in a variety of alternative schemes applied to the linear acoustic system. For the present scheme, such initial data are of course perfectly preserved. Moreover, when the fully nonlinear Euler equations are used, the initial data are almost perfectly preserved by the rotated Richtmyer scheme, which is a natural generalization of our scheme to this problem.

As a final remark, we wish to draw to the attention of our readers the work of Hyman and Shashkov (see [19, 20] and the references cited therein) with which our analysis has many points of similarity. They construct discrete operators on logically rectangular meshes that obey discrete analogues of the major vector identities, such as $CURL \times GRAD = 0$, which is another way of expressing what we do here. The starting points, and the style, of the two analyses are quite different, and although our results are less specific in one sense, being limited to the single identity above, they are more general in the sense of extending to (some) unstructured and multidimensional grids. An extended comparison of the two approaches may well prove profitable.

Appendix. Vorticity production by a general scheme. We consider a class of schemes that include Lax–Wendroff schemes and compute the vorticity that they generate. The schemes are written as (only the velocity updates are needed)

$$u^{n+1} = u^n - \nu\delta_x P - \nu\delta_y Q', \tag{57}$$

$$v^{n+1} = v^n - \nu\delta_x P' - \nu\delta_y Q, \tag{58}$$

where

$$\begin{aligned}
P &= [a + (1-a)\mu_y^2]\mu_x p^n - \tfrac{1}{2}\nu[b + c\mu_y^2]\delta_x u^n - \tfrac{1}{2}\nu d\mu_x\mu_y\delta_y v^n,\\
Q &= [a + (1-a)\mu_x^2]\mu_y p^n - \tfrac{1}{2}\nu[b + c\mu_x^2]\delta_y v^n - \tfrac{1}{2}\nu d\mu_x\mu_y\delta_x u^n,\\
P' &= -e\delta_x v^n,\\
Q' &= -e\delta_y u^n.
\end{aligned}$$

Such a scheme is properly centered in time, and hence second-order accurate, if

$$b + c = 1, \qquad d = 1, \qquad e = 0;$$

a particular case is $a = 1, c = 0$, which corresponds to the standard one-step Lax–Wendroff scheme. For the compact vorticity of (12), in general we have

$$\begin{aligned}
\zeta^{n+1} - \zeta^n &= \nu\left\{\mu_x\delta_x\delta_y P - \mu_y\delta_x\delta_y Q + \mu_x\delta_y^2 Q' - \mu_y\delta_x^2 P'\right\}\\
&= \nu\left\{\mu_x^2\delta_x\delta_y[a + (1-a)\mu_y^2]p^n - \mu_y^2\delta_x\delta_y[a + (1-a)\mu_x^2]p^n\right.\\
&\quad -\tfrac{1}{2}\nu[b + c\mu_y^2]\mu_x\delta_x^2\delta_y u^n + \tfrac{1}{2}\nu d\mu_x\mu_y^2\delta_x^2\delta_y u^n\\
&\quad -\tfrac{1}{2}\nu d\mu_x^2\mu_y\delta_x\delta_y^2 v^n + \tfrac{1}{2}\nu[b + c\mu_x^2]\mu_y\delta_x\delta_y^2 v^n\\
&\quad \left. -e\mu_x\delta_y^3 u^n + e\mu_y\delta_x^3 v^n\right\}\\
&= \nu\left\{a(\mu_x^2 - \mu_y^2)\delta_x\delta_y p^n - \tfrac{1}{2}\nu b\delta_x\delta_y(\mu_x\delta_x u^n - \mu_y\delta_y v^n)\right.\\
&\quad \left. +\tfrac{1}{2}\nu(d-c)\mu_x\mu_y\delta_x\delta_y(\mu_y\delta_x u^n - \mu_x\delta_y v^n) - e(\mu_x\delta_y^3 u^n - \mu_y\delta_x^3 v^n)\right\}.
\end{aligned}$$

This formula displays four different mechanisms for vorticity production. For all of their contributions to vanish, we require

$$a = 0, \qquad b = 0, \qquad c = d, \qquad e = 0,$$

and the unique second-order scheme meeting these constraints has

$$a = b = e = 0, \qquad c = d = 1. \tag{59}$$

If we now take Fourier transforms, we have, with the notation of section 5.1,

$$\begin{aligned}\hat{\zeta}^{n+1} - \hat{\zeta}^n = \nu \big\{ & a(s_y^2 - s_x^2)(-4s_x s_y)\hat{p}^n \\ & -\tfrac{1}{2}\nu b(-4s_x s_y)(2\mathrm{i}c_x s_x \hat{u}^n - 2\mathrm{i}c_y s_y \hat{v}^n) \\ & +\tfrac{1}{2}\nu(d-c)(-4s_x s_y)c_x c_y(2\mathrm{i}c_y s_x \hat{u}^n - 2\mathrm{i}c_x s_y \hat{v}^n) \\ & -e(-8\mathrm{i}c_x s_y^3 \hat{u}^n + 8\mathrm{i}c_y s_x^3 \hat{v}^n)\big\}.\end{aligned}$$

As the mesh size h approaches zero, the left-hand side tends to h times the vorticity, $c_x, c_y \to 1, s_x \to k_x h/2, s_y \to k_y h/2$, and hence

$$\begin{aligned}\frac{\hat{\zeta}^{n+1} - \hat{\zeta}^n}{h} \simeq \mathrm{i}\frac{h^2}{2}\left[\nu^2(b+c-d)k_x k_y(k_x \hat{u}^n - k_y \hat{v}^n) + e\nu(k_x^3 \hat{u}^n - k_y^3 \hat{v}^n)\right] \\ +\frac{h^3}{4}a\nu(k_x^2 - k_y^2)k_x k_y \hat{p}^n.\end{aligned} \tag{60}$$

This shows that most first-order members of the family produce vorticity at a rate proportional to h^2, unless $b + c = d$ and $e = 0$. It also shows that most second-order members will produce vorticity at a rate proportional to h^3 unless $a = 0$; note that the standard Lax–Wendroff scheme has $a = 1$. Finally, if also $b = 0$ and $c = d$, there is no vorticity production. This corresponds to the single-parameter family studied in section 5.1.

REFERENCES

[1] P. L. Roe and E. Turkel, *The quest for diagonalization of differential systems*, in Proceedings of the Workshop on Barriers and Challenges in Computational Fluid Dynamics, 1996, ICASE/LaRC Interdiscip. Ser. Sci. Eng. 6, Kluwer, Dordrecht, The Netherlands, 1998, pp. 351–369.

[2] A. Jameson and T. J. Baker, *Multigrid Solution of the Euler Equations for Aircraft Configurations*, AIAA paper 84-0093, Reno, NV, 1984.

[3] R. D. Richtmyer, *A Survey of Difference Methods for Non-Steady Fluid Dynamics*, NCAR Tech. note 63-2, National Center for Atmospheric Research, Boulder, CO, 1962.

[4] R. D. Richtmyer and K. W. Morton, *Difference Methods for Initial-Value Problems*, Interscience, New York, 1967.

[5] P. K. Sweby, *High resolution schemes using flux limiters for hyperbolic conservation laws*, SIAM J. Numer. Anal., 21 (1984), pp. 955–1011.

[6] K. W. Morton and D. F. Mayers, *Numerical Solution of Partial Differential Equations: An Introduction*, Cambridge University Press, Cambridge, UK, New York, 1994.

[7] R.-H. Ni, *Multiple-grid scheme for solving the Euler equations*, AIAA J., 20 (1982), pp. 1565–1571.

[8] P. I. Crumpton, J. S. Mackenzie, and K. W. Morton, *Cell vertex methods for the compressible Navier-Stokes equations*, J. Comput. Phys., 109 (1993), pp. 1–15.

[9] P. D. Lax and B. Wendroff, *Systems of conservation laws*, Comm. Pure Appl. Math., 13 (1960), pp. 217–237.

[10] A. Arakawa, *A computational design for the long-term integration of the equations of atmospheric motion*, J. Comput. Phys., 1 (1966), pp. 119–143.

[11] D. C. Jesperson, *Arakawa's method is a finite-element method*, J. Comput. Phys., 16 (1974), pp. 383–390.
[12] M. Lukáčová-Medvid'ová, K. W. Morton, and G. Warnecke, *Evolution-Galerkin methods for hyperbolic systems in two space dimensions*, Math. Comp., 69 (2000), pp. 1355–1384.
[13] K. M. Peery and S. T. Imlay, *Blunt Body Flow Simulations*, AIAA paper 88-2924, 1988.
[14] M. Pandolfi and D. D'Ambrosio, *Numerical instabilities in upwind methods: Analysis and cures for the "carbuncle phenomenon,"* J. Comput. Phys., 166 (2001), pp. 271–301.
[15] J. J. Quirk, *A contribution to the great Riemann solver debate*, Internat. J. Numer. Methods Fluids, 18 (1994), pp. 555–574.
[16] J. Gressier and J.-M. Moschetta, *On the Pathological Behaviour of Upwind Schemes*, AIAA paper 98-0110, Reno, NV, 1998.
[17] J.-Ch. Robinet, J. Gressier, G. Casalis, and J.-M. Moschetta, *Shock wave instability and carbuncle phenomenon: Same intrinsic origin?*, J. Fluid Mech., 417 (2000), pp. 237–263.
[18] M. van Dyke, *An Album of Fluid Motion*, Parabolic Press, Stanford, CA, 1982.
[19] J. M. Hyman and M. Shashkov, *Natural discretizations for the divergence, gradient and curl on logically rectangular grids*, Comput. Math. Appl., 33 (1997), pp. 81–104.
[20] J. M. Hyman and M. Shashkov, *Adjoint operators for the natural discretizations of the divergence, gradient and curl on logically rectangular grids*, Appl. Numer. Math., 25 (1997), pp. 413–442.
[21] E. Douay and T. Lefebvre, *Schema de calcul numerique preservant la vorticite*, Internal report, Ecole Nationale Supérieure des Arts et Métiers, Paris, 2000.